buildings

MDPI

Article

Optimization Strategies for Underfloor Air Distribution in a Small-Scale Data Center

Fengjiao Yu [1], Hongbing Chen [1,*], Wenqian Wang [2] and Jingjing An [1]

[1] Department of Environment and Energy Engineering, Beijing University of Civil Engineering and Architecture, Beijing 100044, China; yufengjiao@bucea.edu.cn (F.Y.); anjingjing@bucea.edu.cn (J.A.)
[2] Capital Engineering & Research Invorporation Ltd., Beijing 100176, China; wwq18538112770@163.com
* Correspondence: chenhongbing@bucea.edu.cn

Abstract: The development of 5G application technology has led to a rapid expansion in the scale of internet data center rooms and the number of servers. Due to the high heat generation of data center server equipment and the mixing of hot and cold airflows within the rooms, the thermal environment of these rooms fails to meet operational requirements with increasing energy consumption and thermal density. This study utilized the 6SigmaDC software to simulate and analyze the characteristics and existing problems of airflow distribution in a small-scale data center. Based on identified issues with current airflow patterns, two optimization schemes were proposed, analyzing the effects of raised floor height and the closure of aisles on airflow optimization. The return heat index (RHI) was used as an evaluation metric to assess airflow patterns before and after optimization. When the raised floor height was 600 mm, the maximum temperature at the cabinet inlet and outlet were 19.3 °C and 34 °C respectively, which were the lowest, and the RHI value was 0.9622. Compared with unclosed aisles and closed hot aisles, closed cold aisles effectively reduced the cabinet inlet and outlet temperature and increased the RHI. In addition, closed cold aisles increased the air supply temperature from 18 °C to 20 °C, further reducing the energy consumption of the air conditioning system. This study can provide guidance and act as a reference for optimizing airflow design and energy conservation in small data centers.

Keywords: data center; airflow distribution; local airflow of cabinet; CFD simulation; optimization design

Academic Editor: Apple L.S. Chan

Received: 25 December 2024
Revised: 19 January 2025
Accepted: 26 January 2025
Published: 29 January 2025

Citation: Yu, F.; Chen, H.; Wang, W.; An, J. Optimization Strategies for Underfloor Air Distribution in a Small-Scale Data Center. *Buildings* **2025**, *15*, 428. https://doi.org/10.3390/buildings15030428

Copyright: © 2025 by the authors. Licensee MDPI, Basel, Switzerland. This article is an open access article distributed under the terms and conditions of the Creative Commons Attribution (CC BY) license (https://creativecommons.org/licenses/by/4.0/).

1. Introduction

The rapid development of technologies, such as 5G and AI, etc., has led to an increasing density of devices in data centers, also increasing the power consumption of each individual device. If the heat cannot be effectively dissipated, it can cause a reduction in equipment performance or even damage it [1]. A reasonable airflow distribution ensures that cold air is evenly distributed to various equipment areas, avoiding the occurrence of "hot spot" areas. By simulating and optimizing airflow distribution, data centers (DCs) can improve their operational efficiency and ensure higher computing power. Many strategies have been proposed to improve the efficiency and reduce the energy consumption of DC cooling systems, including airflow management [2], natural cooling [3], liquid cool-

ing [4], and cooling management [5]. Among them, airflow management strategy is considered the mainstream method for improving the thermal environment and cooling efficiency of DCs due to its ease of implementation and operation.

According to the different configured rack density, the design methods for effective cooling in the data centers can be divided into room-based cooling, row-based cooling and rack-based cooling [6]. Room-based cooling can be used in small data centers with low power densities of less than 5 kW/rack or less [7–9]. Row-based cooling is mainly used for medium density data centers, where the rack power density reaches 20 kW/rack [10–12]. For high-density racks with rack densities up to 50 kW/rack, the cooling system is integrated into the rack servers, that is, rack-based cooling. Although the air distribution is not limited by the location of the rack servers in this case, the costs associated with cooling also increase [13–15].

Currently, the most commonly used cooling method is room-based cooling. Cold air is sent out by air conditioning static pressure boxes through the raised floor into the cold aisle of the computer room. This air supply type should be reasonably designed to the height of the raised floor, the form of the floor air outlet, the distance between the air conditioner and the cabinet, etc. There are several ways to improve airflow distribution in data centers based on fixed computer room air conditioning units, including raised floor plenums, perforated tiles, and aisle containment [16]. Patankar [17] discussed various factors related to airflow and cooling in raised floor data centers. Zhang et al. [18] obtained a recommended range of heights for raised floors in data centers with different structures through a comparative analysis of 18 different cases. In order to optimize the cooling performance in raised-floor data centers, Song [19] used the application of fan-assisted perforations. The size of the outlet airflow is related to the perforation rate of the perforated floor, and the best airflow uniformity and thermal performance can be achieved when the perforation rate is between 20% and 30% [20]. In order to analyze the dependence of the pressure loss coefficient of perforated tiles on geometric factors and flow parameters, Ling et al. [21] conducted numerical simulations of the flow distribution of perforated tiles using different pore types and flow parameters.

Due to the fact that cabinets are typically arranged in a "face-to-face and back-to-back" configuration, this may result in undesirable mixing of cold and hot airflows. Under this condition, cold/hot aisle containment are proposed to reduce the risk of cold airflow bypass and hot airflow recirculation. Some studies found that the air supply temperature can be increased from 18 °C to 22 °C through aisle containment [22], optimizing the utilization rate of cooling capacity[23]. Enclosing hot and cold aisles can have different effects in different data centers. Sundaralingam et al. [24] found that cold aisle containment can reduce rack inlet temperatures by as much as 40% without affecting the room layout. However, Manganelli et al. [25] noted that compared to cold aisle containment, hot aisle containment can reduce cooling system annual energy costs by 43% and increase annualized PUE by 15%. In order to improve the thermal environment of front racks, Zhang et al. [26] proposed a method of air flow optimization in the cold aisle by using a jet fan to compensate for the low flow of the perforated tile.

Due to the limitations of existing equipment and space, airflow distribution optimization based on room cooling has become the primary choice for energy-saving retrofit of small data centers [27].

In this paper, 6SigmaDC software was used to simulate the airflow distribution of the whole computer room and the local cabinet under the actual project requirements of a data center in Beijing, and we experimentally tested the thermal environment indicators of the data center. Among the optimization methods mentioned above that are commonly used for room-based cooling, the raised floor height is firstly considered under the structural permissible conditions, since the data center uses an underfloor air supply. Secondly,

based on the selected optimal floor height, the impact of closed aisles was analyzed to select the optimization method, because closed aisles are currently one of the most effective methods for retrofitting data centers. Through the research of this project, references can be provided for energy-saving retrofit of small data centers without changing the layout.

2. Research Methodology

2.1. Experimental Testing

2.1.1. Establishment of Geometric Model

The data center is located in Beijing, China. As shown in Figure 1, the dimensions of the room are 14.75 m (L) × 13.75 m (W) × 3.45 m (H), with an underfloor air distribution conditioning system. Three sides of the room are brick walls, while one side is a glass partition adjacent to the corridor. The walls exhibit good insulation performance. Three air conditioning units with the size of 1.8 m (L) × 1.0 m (W) × 2 m (H) are placed inside the room. Each unit has a rated total cooling capacity of 60 kW, sensible cooling capacity of 33.4 kW, and air supply volume of 6.5 m^3/s. The return air inlet is located at the top of each air conditioning unit.

Five rows of cabinets are laid in the equipment room, labeled A to E. Rows A and B consist of 13 cabinets each, while rows C, D, and E contain 14 cabinets each. The dimensions of each cabinet are 1.1 m (L) × 0.6 m (W) × 2 m (H) and they are positioned on a raised floor with a height of 0.45 m. The raised floor includes perforated panels with a 45% open area to serve as air supply outlets, and each perforated panel measures 0.6 m × 0.6 m. The designed air supply temperature is 18 °C with a relative humidity of 50%. The airflow distribution in this data center room follows a down-supply and up-return configuration.

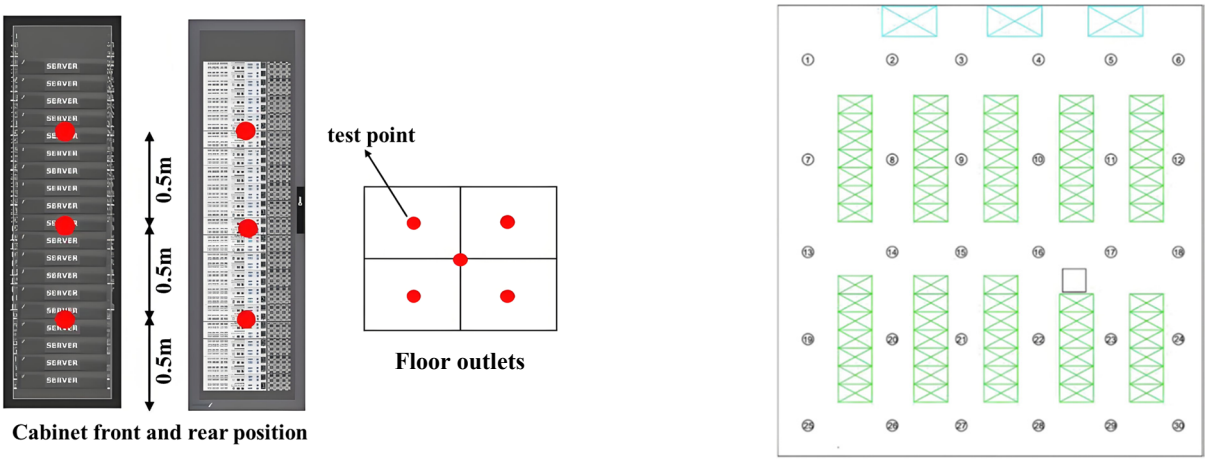


Figure 1. Internal view of the data center.

2.1.2. Description of Experimental Testing

In this study, a hot-wire anemometer was used to experimentally measure the thermal environment conditions of the data center. The experimental testing was divided into two groups. The first group, as shown in Figure 2a, measured the temperature and velocity at the perforated floor outlets and the inlet and outlet of the server cabinets. This group focused on cabinets in rows C and D. For each cabinet, measurements were taken at three points (0.5 m, 1.0 m, and 1.5 m above the floor) at both the front and rear. For the perforated floor outlets, measurements of temperature and velocity were taken by dividing each perforated tile into four equal square sections, with one measurement point at the center of each square and an additional point at the center of the tile. The second group

of tests involved 30 different measurement points distributed within the room, as shown in Figure 2b. Each measurement point was located 1 m above the floor. All results were averaged through three measurements. The temperature and airflow velocity at each testing point were measured using a hot wire anemometer. The temperature range of the anemometer is −20 °C to 70 °C, with an accuracy of ±0.5 °C; correspondingly, the airflow velocity measurement range is 0.02–20 m/s, with an accuracy of 3% of the read value plus 0.03 m/s.



(**a**) Measurement points for cabinets and open floor outlets (**b**) Test points in the room

Figure 2. Distribution of measurement points for cabinets\open floor outlets and test points in the room.

2.2. Numerical Method and Boundary Conditions

The physical model was established by using 6SigmaDC software, which is a mainstream CFD software for analyzing the airflow characteristics and energy consumption of a data center. At present, the software has been widely used and its accuracy has been verified [28,29]. The cabinet models used in the simulation are consistent with the actual parameters, which increases the accuracy of the results. The standard k-ε turbulence model was selected for numerical simulation. In order to improve the computational speed and accuracy, reasonable assumptions were made to simplify and optimize the simulation while meeting all required conditions. The assumptions were as follows:

(1) The large-scale airflow within the room with limited pressure variations was assumed to satisfy the Boussinesq hypothesis. (2) The airflow was regarded as incompressible viscous fluid flow. (3) The heat dissipation caused by fluid viscous forces was neglected. (4) The computer room was regarded as an adiabatic room where the maintenance structure with excellent thermal insulation was unaffected by external conditions. (5) The heat generated by the cabinets was considered as constant across both time and space. (6) The influence of cables and other obstructions in the plenum chamber on the pressure distribution was ignored.

To ensure the accuracy of the simulation results, a grid independence test was conducted using three different grids (1,295,000; 4,838,000; and 7,835,000 grid elements). The control equations were solved in 6SigmaDC under identical conditions. By observing the computer room temperature contours and the monitoring points, it was found that there was no significant deviation in the results under different grids, which confirmed the grids' independence of the simulation results. Therefore, 1,295,000 grids were adopted for the simulation.

Meanwhile, the operating parameters for the air conditioning units and IT equipment were from the actual operational and experimental measurement data of the data center.

The air conditioning supply and return air outlets were treated as free openings, while the perforated floor model ignored its thickness. The boundary conditions are shown in Table 1.

Table 1. Boundary conditions.

Parameters	Boundary Conditions
Air Volume (m^3/s)	8.5
Supply Air Temperature (°C)	18
Heat Dissipation of Cabinet (kW)	See Table 2
Wall, Floor, and Ceiling	Adiabatic Boundary
Perforated Floor Porosity	45%

Different numbers of racks in the cabinet resulted in different heat dissipation powers of each cabinet. Therefore, the heat dissipation of each cabinet was calculated based on the measured temperature difference between the cabinet's inlet and outlet, and this value was used as the heat source boundary condition. The specific data are shown in Table 2."/" indicates that the rack in the cabinet is not in use.

Table 2. Power of each cabinet (kW).

No.	1	2	3	4	5	6	7	8	9	10	11	12	13	14
A	2.00	0.38	0.65	1.76	1.69	1.69	/	3.50	5.50	3.50	2.07	0.78	1.21	1.45
B	/	0	0	0	0	0	/	/	0.78	0.30	0.35	0.52	0.15	1.55
C	2.00	1.25	0.88	0.60	2.40	1.77	0.98	095	2.50	0.96	2.40	0.20	0.35	0.66
D	/	2.00	1.03	1.23	3.866	2.86	1.89	/	2.93	1.96	0.40	1.45	1.50	0.73
E	0.35	0.62	0.80	0.58	0.60	1.04	0.35	4.40	6.07	0.60	0.70	1.56	0.90	0.30
Total Power of the Cabinet											90.47			

2.3. Thermal Environment Evaluation Indicators

Cho et al. [30] defined four cooling performance metrics to comprehensively evaluate the cooling efficiency, that is, the Supply/Return Heat Index (SHI/RHI), the Rack Cooling Index (RCI), and the Return Temperature Index (RTI). In this study, the RHI was selected to evaluate the thermal environment of the data center. The RHI represents the degree of mixing cold air supply and hot return stream. An RHI value closer to 1 indicates less mixing of hot and cold air, signifying higher efficiency of the air conditioning supply. The RHI calculation formula is shown below [31]:

$$\mathrm{RHI} = \frac{Q}{Q + \delta Q} = \frac{\sum_j \sum_i m_{i,j} c_p \left(\left(T_{out} \right)_{i,j} - \left(T_{in} \right)_{i,j} \right)}{\sum_j \sum_i m_{i,j} c_p \left(\left(T_{out} \right)_{i,j} - T_{ref} \right)} \quad (1)$$

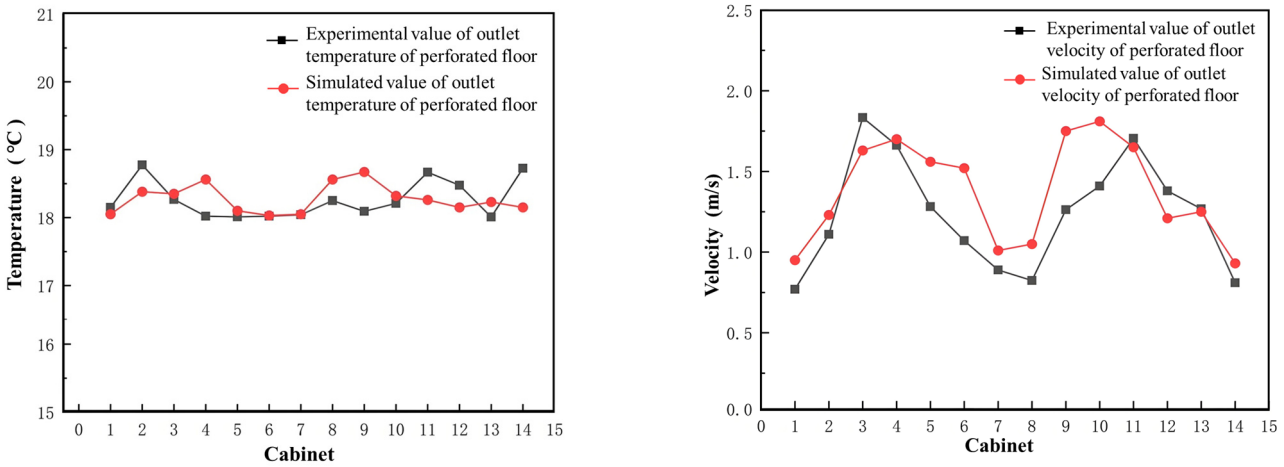
where: Q (kW) represents the total heat dissipation of all cabinets in the data center; δQ (kW) denotes the enthalpy increment before the air supply enters the cabinet; $m_{i,j}$ (kg/s)is the mass flow of air through each cabinet; $(T_{in})_{i,j}$ and $(T_{out})_{i,j}$ represent the average inlet and outlet temperatures of each cabinet (°C); T_{ref} (°C) is the air supply temperature at the air conditioning unit; and C_p (kJ/(kg·K)) is the constant pressure specific heat capacity of air.

3. Results and Discussion

3.1. Validation of Experimental and Simulation Results

Figure 3 shows the measured and simulated values of airflow velocity and temperature at the perforated floor outlets. In Figure 3a, the largest experimental and simulation

errors occurred in cabinets 4 and 9, followed by cabinets 14 and 12, which were 3.33%, 3.31%, 2.67%, and 2.13%, respectively. The main reason was that the power supply in the cabinets and the cables under the floor affected the temperature distribution. However, it can be observed that the experimental and simulated temperature values at the perforated floor outlets maintained a consistent trend, with an average relative error calculated at only 2%. Figure 3b indicates that cabinets 1 to 7 were located in the same cold aisle, as were cabinets 8 to 14, both exhibiting similar trends. The airflow velocity at the perforated floor grille outlets within the cold aisle initially increased and then decreased, with certain sections showing a sharp decline, possibly due to vortices formed within the plenum. The overall trend in air flow velocity was similar, with an average relative error of 18%. However, in actual operation, cabinets 1 and 8 in each row served as UPS units, and cabinets 6 and 9 experienced airflow obstruction due to cables beneath the raised floor, leading to a decrease in outlet airflow velocity. This obstruction resulted in a larger discrepancy between the simulated and experimental values. Excluding the error from these four cabinets, the adjusted average relative error was 12%.



(a) Experimental and simulated values of temperature (b) Experimental and simulated values of velocity

Figure 3. Experimental and simulated values of temperature and velocity at the perforated floor outlets.

Figure 4 shows the outlet temperature values at a height of 1 m above the floor for each cabinet. Meanwhile, the standard deviation is represented by error bars in Figure 4, which clearly shows that the overall experimental data has a relatively small degree of dispersion. A comparison between the experimental and simulated values revealed a generally similar trend. However, there was a noticeable temperature variation at the cabinet outlets in different locations. This is due to differences in the number of servers across cabinets in the actual data center, resulting in significant variations in power output. Therefore, with the same air supply temperature, the outlet temperature for each cabinet primarily depends on the scale of servers within the cabinet. Additionally, for cabinets 1 and 2, which are farther from the air conditioning units, the simulated values are notably higher than the experimental values. This discrepancy arises because the servers in these two cabinets are positioned at the base, whereas the experimental data represents outlet temperatures measured at a height of 1 m above the floor. Consequently, the simulated outlet temperature is higher than the experimental value, with an average relative error of 5.7%.

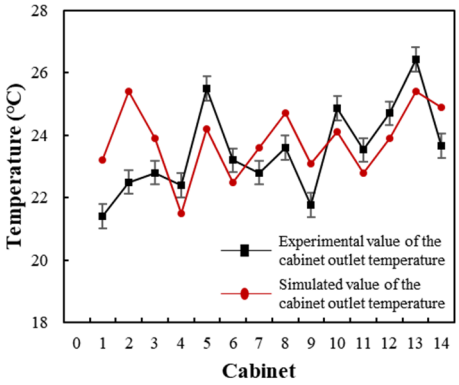
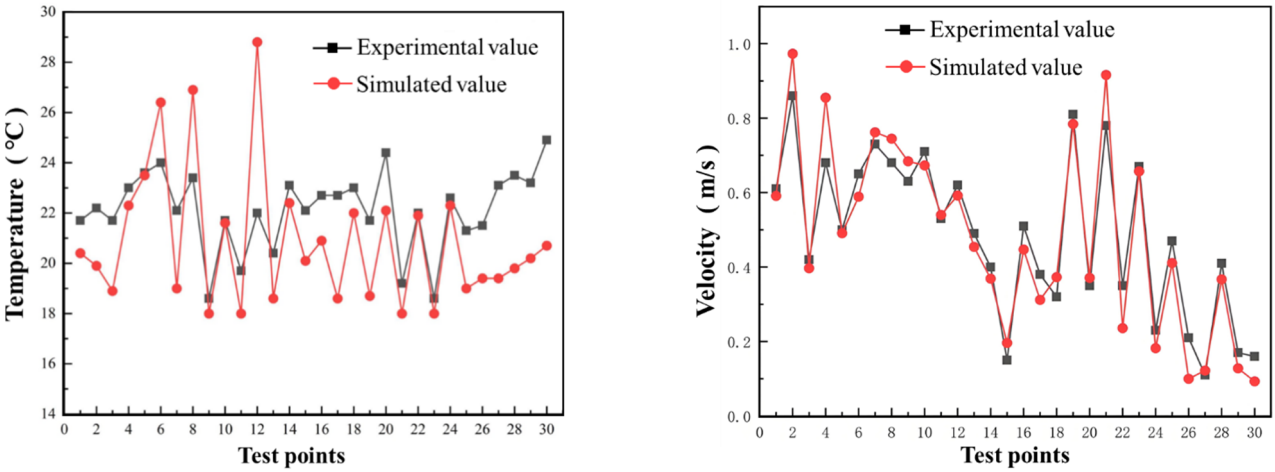


Figure 4. Experimental and simulated values of the cabinet outlet temperature.

Figure 5 presents the experimental and simulated values of temperature and airflow velocity at test points located 1 m above the floor in the data center. It shows a generally consistent trend between the two, with a maximum temperature difference of 7 °C and a maximum airflow velocity difference of 0.175 m/s between the experimental and simulated values. The calculations indicate an average relative error of 9.44% for temperature and 12.6% for airflow velocity, both meeting the requirement that the average relative error should not exceed 15% [32].



(a) Experimental and simulated values of temperature (b) Experimental and simulated values of velocity

Figure 5. Experimental and simulated values of temperature and velocity at different locations in the data center.

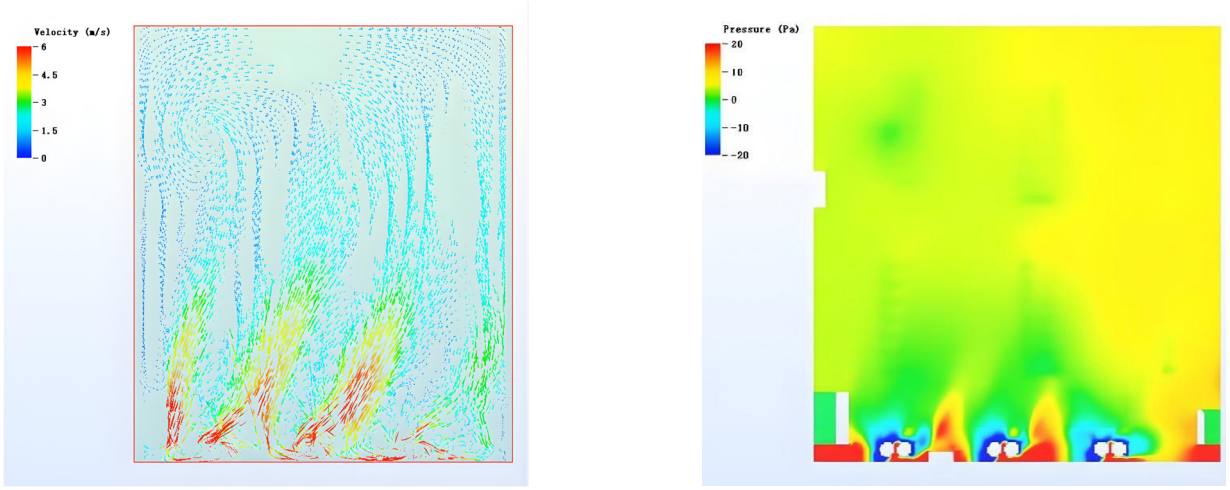
The data center used for this experiment is an actual engineering facility, not a strictly controlled laboratory environment, and there were unavoidable factors that may have influenced the experimental results. For example, variations in server power and human testing error could affect the data obtained. Figure 3 to Figure 5 demonstrate that the CFD model established in this study for the data center exhibits a similar trend to the experimental results, with errors within the range of 2% to 12.6%. Based on these results, the CFD model developed in this study for the data center is considered to have a certain degree of reliability and accuracy, making it suitable for subsequent simulation and optimization research.

3.2. Analysis of Data Center Thermal Environment Simulation Results

3.2.1. Airflow Distribution Within the Floor Plenum

The cold air processed by the air conditioning system flows through the floor plenum and the perforated raised floor to reach the cabinet inlets, thereby achieving cabinet cooling. The pressure distribution and flow characteristics at various locations within the floor plenum significantly affect the air supply and airflow distribution in the entire data center. Therefore, the pressure contour and flow streamlines within the floor plenum can be used for analysis. Figure 6a shows the airflow streamlines and velocity distribution within the floor plenum. As illustrated, beneath the cold aisle near the air conditioning unit, the primary airflow from the air supply outlet carries the surrounding airflow through the perforated floor into the cold aisle. However, in areas farther from the air conditioning units, increased resistance and reduced airflow velocity result in the formation of a vortex on the left side, with the vortex center located at the end of the cold aisle.

Figure 6b shows the pressure contour at 0.25 m below the floor within the plenum. As observed, the overall pressure distribution is uneven. The pressure gradually increases with the distance from the cabinets; however, in the vortex region farther from the air conditioning units, the pressure shows a decreasing trend. Consequently, the relatively low static pressure in the distal end of the plenum, compared to the end near the air conditioning units, can hinder effective air supply to the far end cabinets.



(a) Velocity vector diagram in the plenum chamber (b) Pressure contours in the plenum chamber

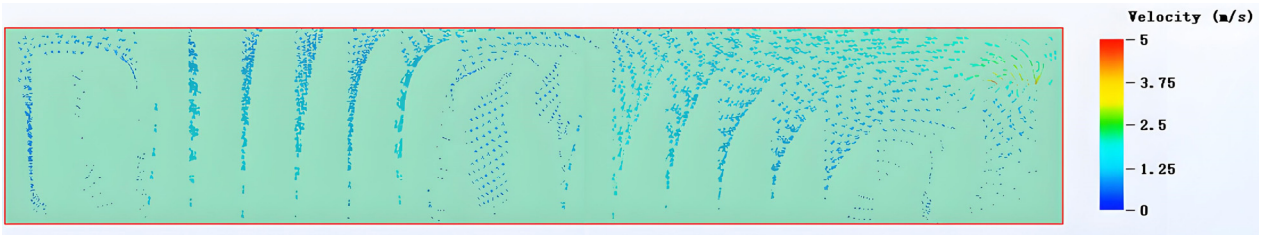
Figure 6. Velocity vector diagram and pressure contours in the plenum chamber.

3.2.2. Airflow Distribution Within the Cold Aisle

Figure 7a shows the velocity vector distribution on a vertical cross-section within the cold aisle between cabinets C and D. As observed, the airflow direction is vertical to the floor and flows upward when the airflow flows out of the floor grille outlet. In the cold aisle away from the air conditioning unit, the airflow primarily maintains its upward direction. However, in the cold aisle near the air conditioning unit, a horizontal velocity component is clearly visible. This is due to the low ceiling, which restricts the airflow, causing some air to recirculate and form a vortex in this region. The vortex within the cold aisle reduces the volume of airflow reaching the cabinet inlets, resulting in inlet temperatures that exceed the supply air temperature, thereby preventing adequate cooling and potentially impacting the long-term stable operation of the equipment.

Figure 7b shows the temperature contour at the same location as in Figure 7a. The color distribution indicates that the temperature within the cold aisle area is generally consistent with the air supply temperature of 18 °C. However, in the vortex region near

the air conditioning unit, a noticeable temperature increase is observed, reaching up to 19.3 °C. This temperature rise can be attributed to two factors: first, the mixing of airflows; and second, the conversion of kinetic energy into internal energy due to viscous forces within the vortex, leading to an increase in the surrounding air temperature.



(a) Velocity vector diagram in the cold aisle



(b) Temperature contour in the cold aisle

Figure 7. Velocity vector diagram and temperature contour in the cold aisle.

Figure 8 illustrates the airflow distribution at the perforated floor grille outlets in the data center. The outlets near the air conditioning unit and at the end of the cold aisle exhibit lower airflow rates. This is because of the higher airflow velocity near the air conditioning unit, resulting in lower pressure within the floor plenum in this region. Additionally, airflow vortices tend to form at the end of the cold aisle, leading to an uneven distribution of airflow across the floor grilles. Specifically, cabinets 14 in rows A, B, C, and D are at disadvantageous points for air supply, with cabinet 14 in row D having the lowest airflow rate of 0.08 m/s, significantly lower than the flow rates in the central region.

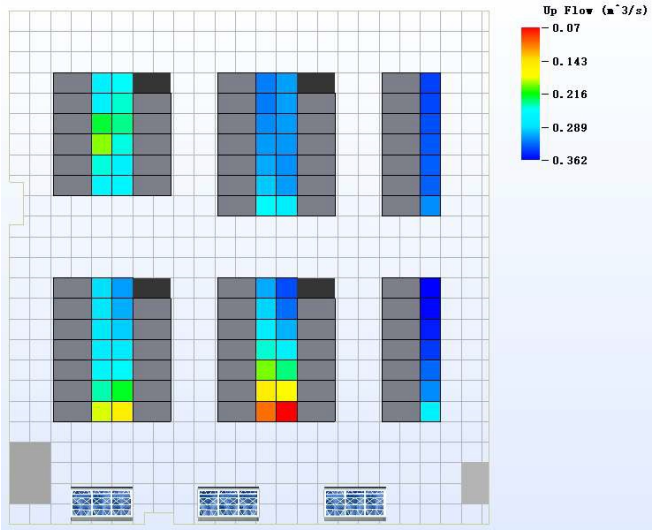


Figure 8. Flow contours of perforated floor outlets.

3.2.3. Airflow Distribution Within the Hot Aisle

The hot aisle is a closed area located behind the cabinets, separated from other parts of the room. Airflow from the rear of the cabinets mixes before returning to the air conditioning unit, resulting in a relatively large temperature gradient within the hot aisle. Figure 9 shows the velocity vector distribution in the hot aisle outside rows C and D. As illustrated, the exhaust airflow from the cabinet outlets undergoes thorough mixing, with some turbulent flow phenomena leading to recirculation toward the cold aisle. It can be observed that the airflow near the cabinet exhaust outlets does not flow in a unidirectional manner; rather, there are interactions present that create complex airflow patterns. This may result in less than ideal airflow within the cold aisle, subsequently affecting the overall cooling efficiency of the data center.

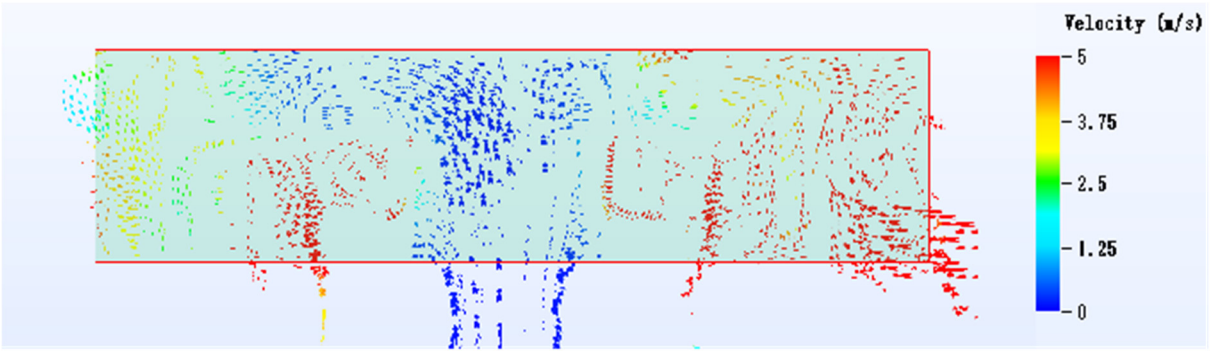


Figure 9. Velocity vector diagram of hot aisles.

Figure 10 shows the horizontal temperature contour at a height of 1 m above the floor. Due to variations in the number of IT devices within each cabinet, the heat dissipation also differs, resulting in a random distribution of outlet temperatures across the cabinets. Each cabinet outlet exhibits a different temperature, with redder colors indicating higher temperatures. The random distribution of cabinets with varying heat dissipation affects the overall airflow distribution and thermal environment within the data center.

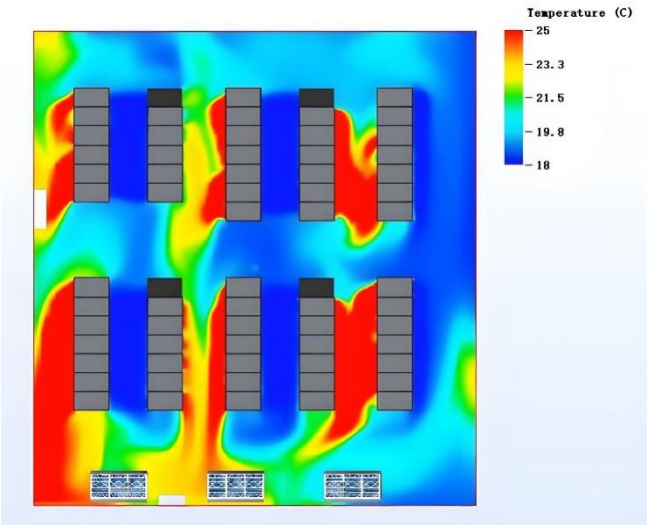


Figure 10. Temperature contours at a height of 1 m from the floor.

4. Airflow Distribution Optimization Strategy

When air conditioning units in a data center use perforated floor grilles for underfloor air distribution, several issues arise, including uneven pressure distribution within

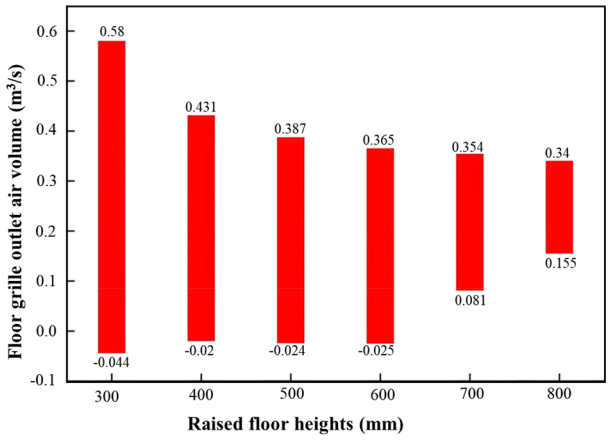
the floor plenum, non-uniform airflow through the perforated floor, and vertical temperature gradients within cabinets. These issues can lead to disorganized airflow, localized hot spots in cabinets, and compromised operation of server equipment. Based on this, this study investigated the effects of two different optimization schemes on airflow distribution: varying the raised floor heights, and closed cold/hot aisles. The SHI evaluation index was used to quantitatively analyze the mixing of hot and cold air under different influencing factors, aiming to meet operational requirements for cabinet servers, reduce data center air conditioning system energy consumption, and prevent undercooling or overcooling of cabinets.

4.1. Raised Floor Height Adjustment

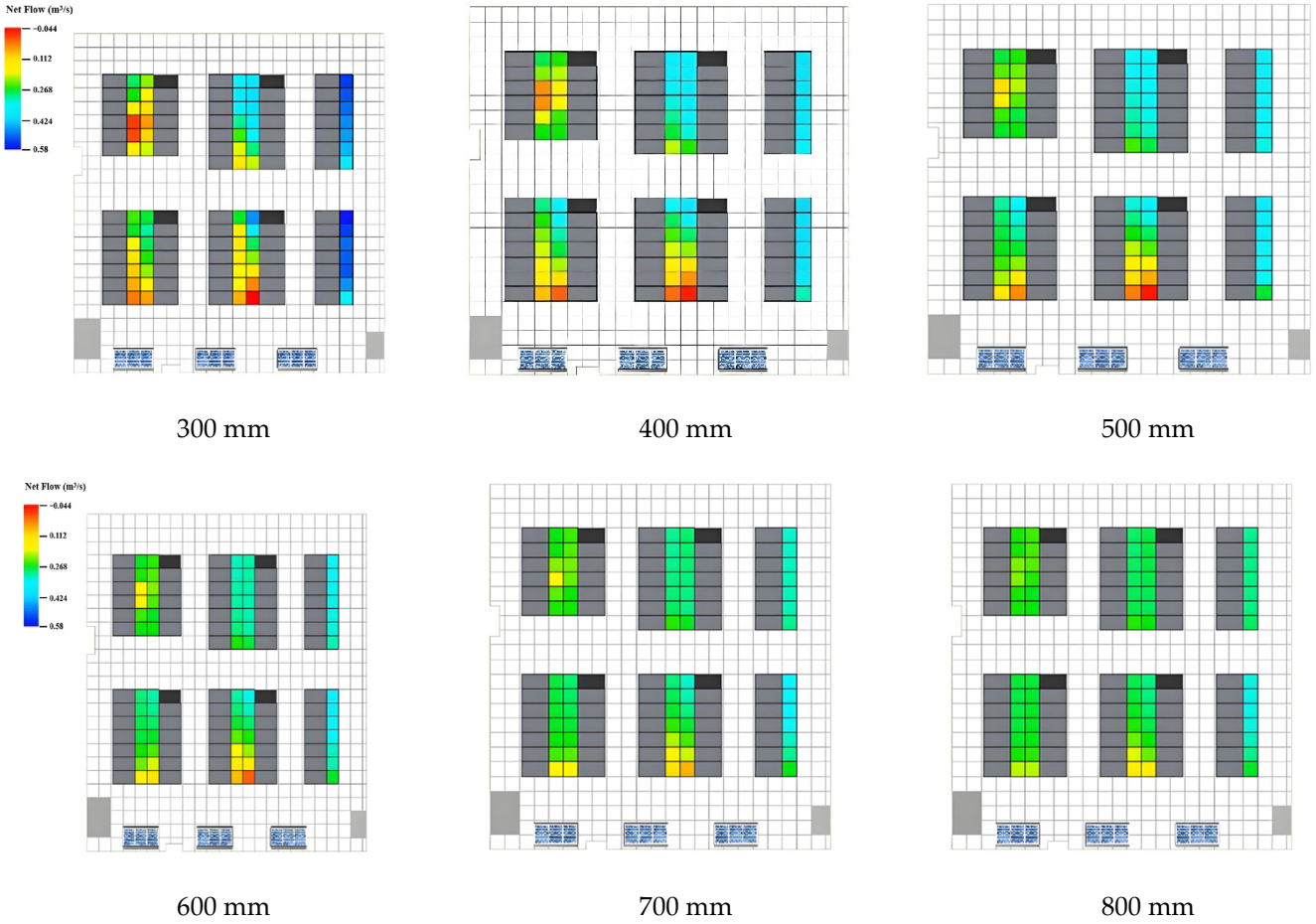
Different raised floor heights can alter the inlet airflow volume to the server cabinets, affecting the velocity and pressure distribution within the underfloor plenum, and consequently influencing the cooling performance of the server equipment. This study's airflow distribution optimization plan included a total of six groups of raised floor heights ranging from 300 mm to 800 mm, varied in steps of 100 mm, simulating the optimization effects on airflow distribution within the data center at various floor heights.

4.1.1. Airflow Volume Analysis

Figure 11a illustrates the distribution range of airflow volume at the perforated floor grilles under different raised floor heights. As shown, at a raised floor height of 300 mm, the airflow volume range was −0.044 m³/s to 0.58 m³/s. As the raised floor height increased, the differences in airflow volume distribution at the perforated floor grilles in the data center decreased, which means a better airflow volume uniformity. At a height of 800 mm, the airflow volume range was 0.155 m³/s to 0.34 m³/s. To facilitate subsequent analysis and comparison of the airflow volumes at the perforated floor grilles under different raised floor heights, the outlet airflow volume at 300 mm was used as a standardized reference range. The outlet airflow volumes at various raised floor heights within this range are depicted in Figure 11b.



(a) Outlet airflow volume range at different raised floor heights



(b) Outlet airflow contours at different raised floor heights

Figure 11. Outlet airflow volume range and contours of floor grilles at different raised floor heights.

From Figure 11b, it can be observed that as the raised floor height increased, the airflow volume at the perforated floor grilles gradually increased, and the disparity in airflow volume at the grilles also continued to diminish. When the height was increased from 300 mm to 500 mm, negative values for the airflow volume were observed at the grilles closer to the air conditioning side. As mentioned above, the minimum airflow volume for a 300 mm raised floor height is −0.044 m^3/s. Similarly, the minimum airflow volume is −0.02 m $^3/s$ and −0.024 m^3/s for 400 mm and 500 mm raised floor heights. These results indicate that the closer the grille is to the air conditioning unit, the lower the outlet airflow volume, which is consistent with the conclusions presented in Figure 8. This discrepancy is attributed to the uneven pressure distribution within the underfloor plenum. Meanwhile, there is a hot and cold aisles arrangement in the data center room, which is not closed, and the cold airflow will flow back into the hot aisle, resulting in a phenomenon of mixing cold and hot air. When the raised floor height increases from 600 mm to 800 mm, there are no negative values for the airflow volume at the floor grilles and the airflow volume range is −0.025 m^3/s–0.58 m^3/s for a 600 mm raised floor height, 0.081 m^3/s–0.354 m^3/s for 700 mm, and 0.155 m^3/s–0.34 m^3/s for 800 mm. It can be clearly seen that the difference in airflow volume between the grilles near the air conditioning unit and those at the far end gradually decreases, from 0.34 m^3/s to 0.18 m^3/s gradually when the floor's raised height increases from 600 mm−800 mm. The distribution range of airflow volume becomes more concentrated compared to the previous heights, indicating that at this raised floor height, the outlet airflow from the floor grilles is relatively uniform. When the raised floor height reaches 800 mm, the changes in airflow volume at the grilles are not

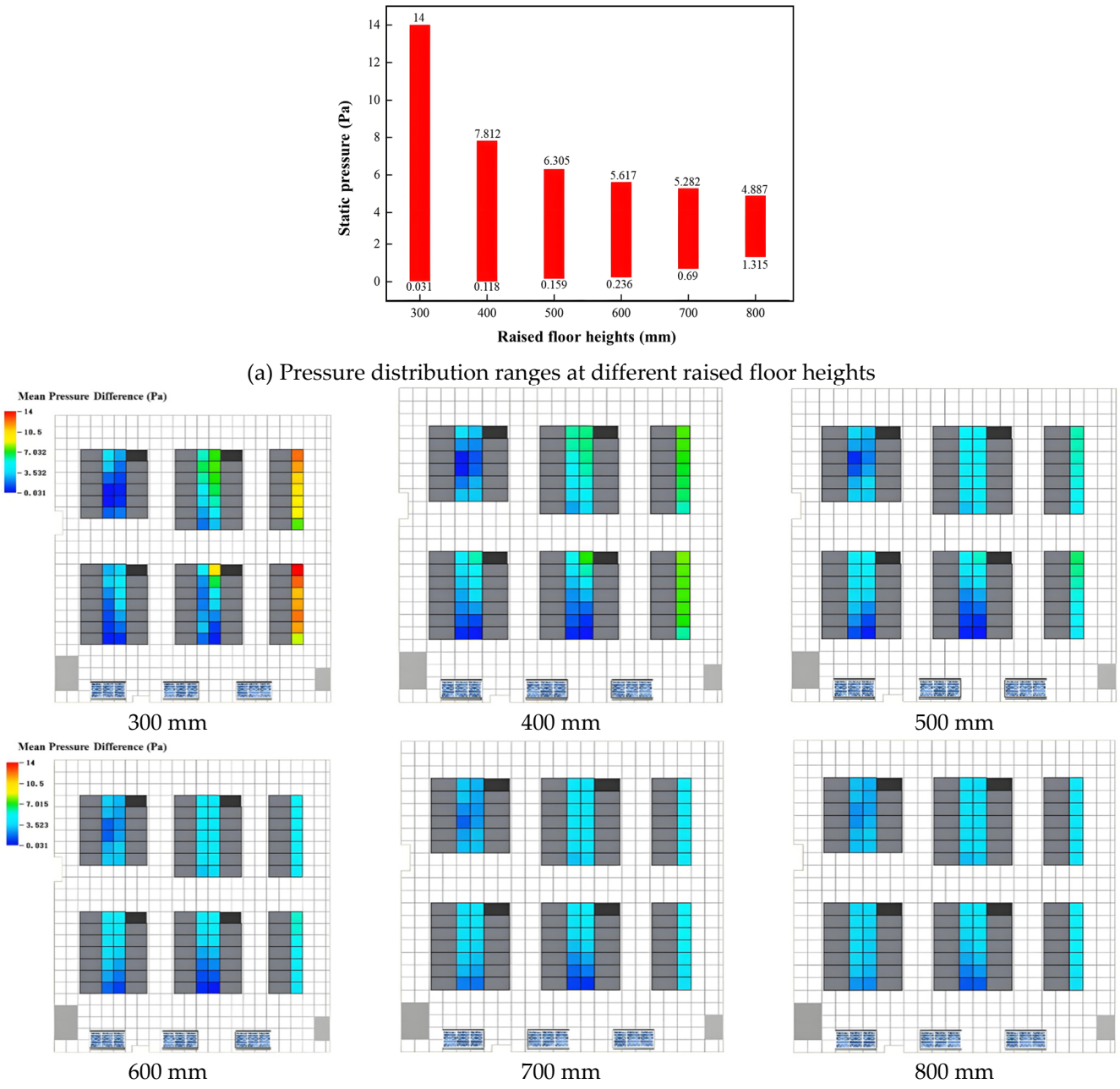
significantly different from previous heights, suggesting that further increasing the raised floor height beyond 800 mm may not effectively improve the airflow volume at the grilles.

The simulation results of airflow volume distribution at the perforated floor grilles under different raised floor heights indicate that as the height increases, the airflow volume becomes increasingly uniform, effectively addressing the mismatch between the outlet airflow from the grilles and the required airflow for the cabinets. The optimal height range is between 600 mm and 800 mm, during which the outlet airflow best meets the requirements. When the height is below 600 mm, some perforated floor grilles may exhibit negative airflow values, while increases beyond 800 mm yield minimal improvement.

4.1.2. Pressure Field Analysis

The horizontal pressure distribution in the underfloor plenum affects the uniformity of the supply airflow distribution, which in turn impacts the airflow distribution within the data center. Figure 12a illustrates the pressure distribution range between the perforated floor grilles and the floor plane at different raised floor heights. At a raised floor height of 300 mm, the static pressure zone has the highest value, ranging from 0.031 Pa to 14 Pa. To facilitate the analysis and comparison of the static pressure distribution between the floor grilles and the floor plane at different raised floor heights, the static pressure distribution range at a height of 300 mm was used as a standardized reference range. It can be observed from the figure, as the raised floor height increases, the differences in static pressure between the perforated floor grilles and the floor plane within the data center decrease progressively.

Figure 12b presents the pressure distribution contours between the perforated floor grilles and the floor plane at different raised floor heights. It is evident that as the height of the raised floor increases, the static pressure between the floor grilles and the floor plane gradually decreases. At the same raised floor height, the static pressure at the outlets of the floor grilles near the air conditioning units is lower compared to other locations. When the raised floor height increases from 300 mm to 600 mm, the static pressure distribution at the floor grille outlets becomes increasingly uniform and the static pressure difference decreases from 13.969 pa to 7.694 pa and 6.146 pa, respectively. This is particularly noticeable at the outlets of the floor grilles for the cabinets in row E, where the pressure variations become more consistent. When the raised floor height increases from 600 mm to 800 mm, the static pressure distribution at the floor grille outlets remains basically unchanged, and the improvement in the uniformity of the static pressure distribution between the floor grilles and the floor plane is minimal. The static pressure at the floor grille outlets determines the airflow volume; a higher static pressure facilitates the flow of supply air from the underfloor plenum into the cold aisle area of the data center. Consequently, the airflow volume at the cold aisle grilles near the air conditioning units is relatively smaller than that at other locations, which is consistent with the findings of the airflow analysis.



(a) Pressure distribution ranges at different raised floor heights

(b) Pressure distribution contours at different raised floor heights

Figure 12. Pressure distribution ranges and contours at different raised floor heights.

To investigate the uneven airflow and pressure at the outlets of the floor grilles in the cold aisle near the air conditioning unit, horizontal pressure distribution contours within the plenum below the floor plane at a height of 0.2 m were obtained at different raised floor heights, as shown in Figure 13. When the raised floor height is 300 mm or 400 mm, the blue areas under the floor grilles in the cold aisle near the air conditioning unit are noticeably prominent, indicating significant negative pressure in this region, which hampers the supply airflow from the plenum into the cold aisle, resulting in reduced airflow at the floor grille outlets. Conversely, the red areas beneath the floor grilles farther from the air conditioning unit are clearly visible, indicating higher pressure in this region, leading to increased airflow at the floor grille outlets. The overall pressure distribution within the plenum at this raised floor height is extremely uneven, and the pressure distribution along the cold aisle in the data center is also irregular. As the raised floor height increases from 500 mm to 800 mm, the blue area near the air conditioning unit gradually diminishes

in size and intensity, indicating an improvement in the static pressure at the floor grille outlets near the air conditioning unit. Meanwhile, the red area farther from the air conditioning unit gradually disappears, indicating a decrease in static pressure within the plenum. Once the raised floor height reaches 600 mm, the horizontal pressure distribution within the plenum remains largely unchanged, suggesting that further increases in the raised floor height do not significantly affect the horizontal pressure within the floor plenum.

The primary reason for the lower static pressure at the floor grille outlets in the area near the air conditioning unit is that the direction of the supply airflow from the air conditioning unit is perpendicular to the airflow direction at the floor grille outlets. According to Bernoulli's principle, the closer one is to the air conditioning unit, the faster the supply airflow velocity, resulting in lower static pressure in that area. This low static pressure makes it difficult for airflow to enter the cabinets close to the air conditioning unit, causing the airflow to move away from this region at a higher velocity, thereby resulting in a smaller airflow volume at the floor grille outlets near the air conditioning unit.

From the above analysis, it is evident that variations in the raised floor height can affect the horizontal static pressure distribution within the underfloor plenum. As the raised floor height increases, the uneven pressure distribution within the plenum improves, leading to a more effective airflow supply. When the raised floor height is low, it is advisable to avoid placing cabinets near the air conditioning unit; instead, positioning them slightly farther away can better meet the cooling requirements of the servers within the cabinets and prevent overheating.

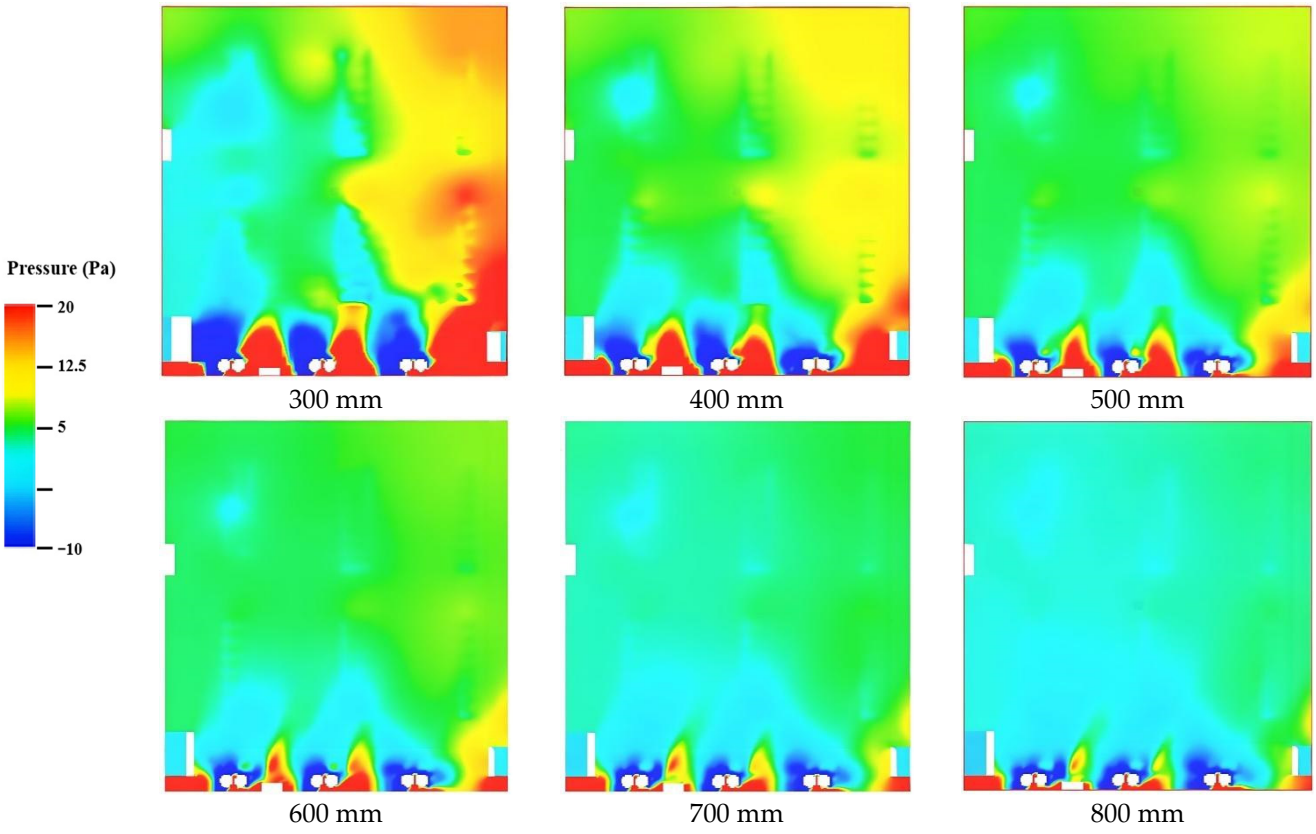


Figure 13. Horizontal pressure distribution contours at 0.2 m below the floor at different raised floor heights.

4.1.3. Temperature Field Analysis

It should be pointed out that the airflow distribution ultimately affects the overall heat exchange process in the data center, resulting in variations in the temperature field. Therefore, the three cross-sectional areas for a temperature field simulation of the data center and cabinets at different raised floor heights, which are the bottom section (0.2 m), the middle section (1.0 m), and the top section (1.8 m), were selected. This simulation provides temperature values at different heights and the inlet and outlet temperatures of the cabinets. Notably, the minimum temperature at all three cross-sectional locations remains constant at 18 °C, while only the maximum temperature at each section varies. The maximum temperature changes at the three cross-sections are illustrated in Figure 14.

As shown in Figure 14, when the raised floor height increases from 300 mm to 600 mm, the temperature at the bottom of the data center decreases with the elevation of the raised floor, while the middle temperature gradually declines. However, after reaching a height of 500 mm, the temperature at the top of the data center begins to rise. This is mainly due to the fact that as the height of the raised floor increases, the distance between the top of the cabinet and the ceiling decreases. This restricts the free flow of hot air in the room, leading to a severe mixing of hot and cold air currents and resulting in an increase in the maximum temperature. When the height continues to increase above 600 mm, the temperature at the bottom decreases and then increases, showing fluctuations, while the temperature in the middle increases and then decreases, also showing fluctuations. The temperature at the top continues to increase, but the growth rate is decreasing. In summary, when the raised floor height exceeds 600 mm, the temperature distribution is not ideal.

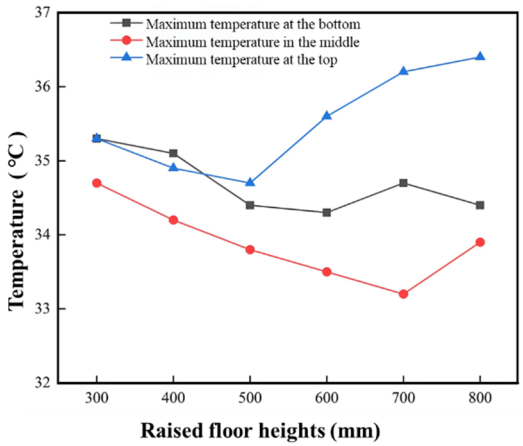


Figure 14. Maximum temperature variation of sections with different raised floor heights.

To better understand the variations in cabinet temperatures, Figure 15 illustrates the distribution of average inlet and outlet temperatures for the cabinets. It can be observed that as the raised floor height increases, the minimum inlet and outlet temperatures remain relatively constant, while the maximum temperatures show a significant decrease. When the height reaches 600 mm, the maximum temperature at the cabinet inlet and outlet are 19.3 °C and 34 °C, respectively, and the difference between the maximum and minimum temperatures continues to diminish. However, as the height is increased further, this difference exhibits fluctuations, indicating that increasing the height has a limited impact on the temperature field at this point. As the raised floor height increases, the maximum cabinet inlet temperature initially rises and then decreases, while the minimum value remains relatively constant. This behavior is attributed to the presence of a high-temperature air mass at a height of 400 mm, causing an increase in temperature, with the

highest temperature reaching up to 21.2 °C. The minimum value of the cabinet outlet temperature remains around 32.8 °C, while the maximum value shows a trend of first decreasing and then increasing as the raised floor height increases. The trend in the temperature difference between the inlet and outlet of the cabinets remains consistent.

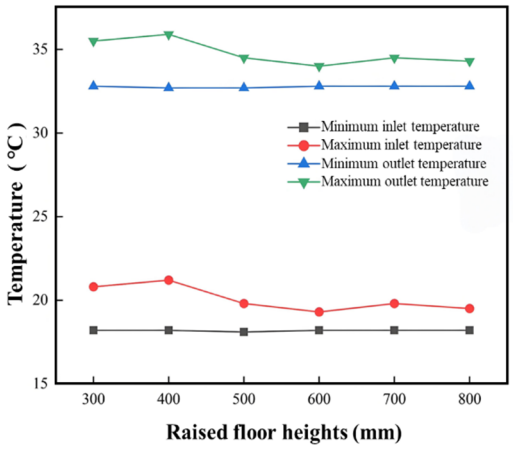
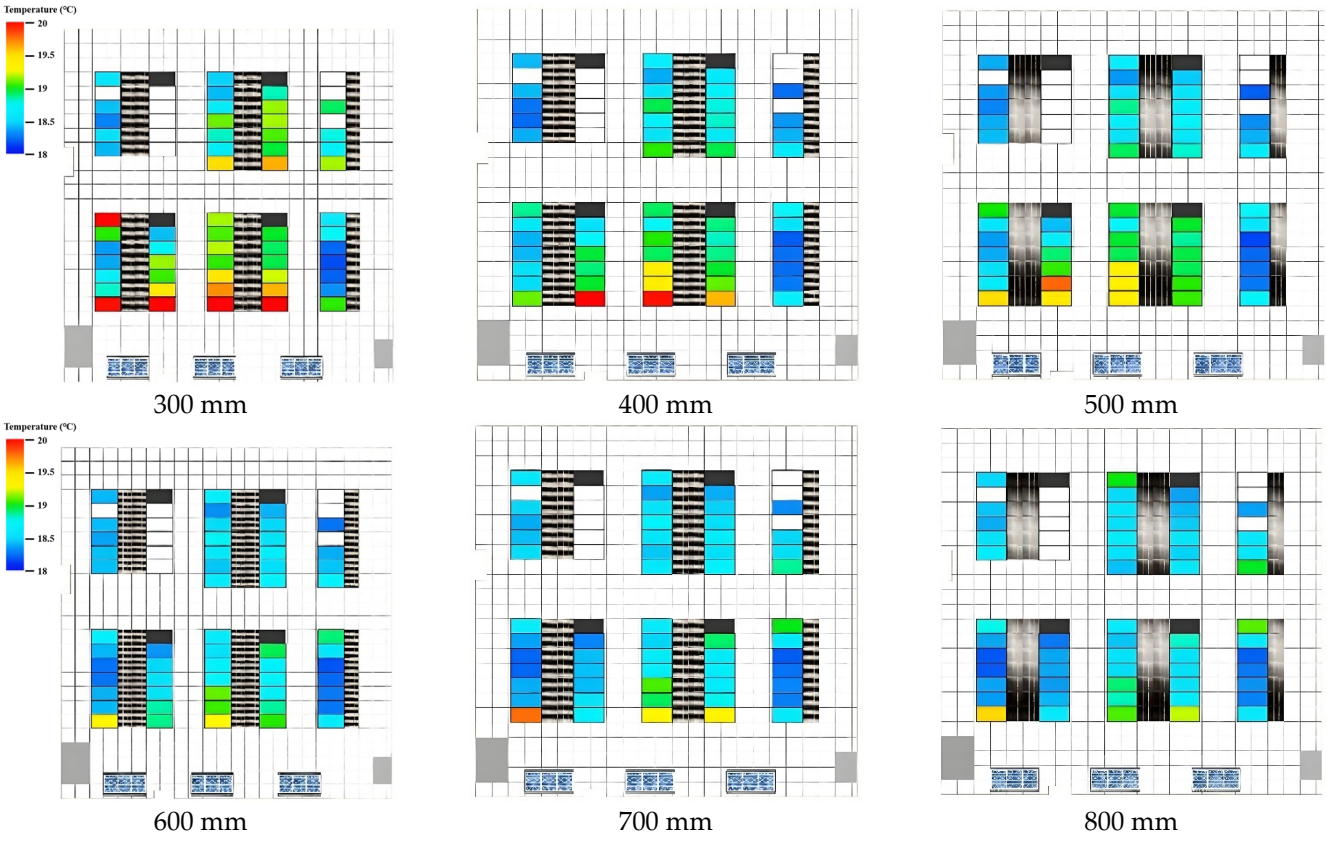


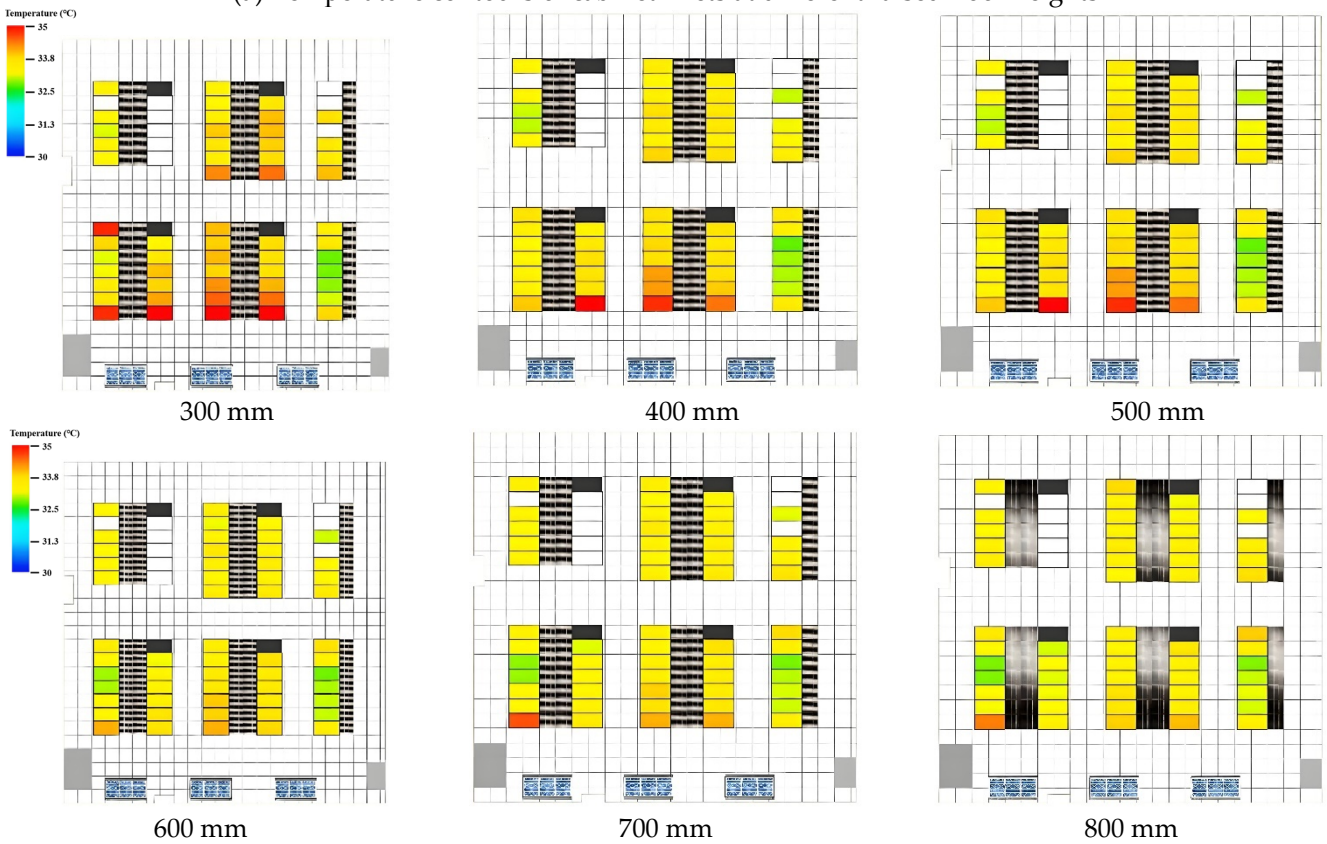
Figure 15. Temperature distribution of cabinet inlets and outlets for different raised floor heights.

Figure 16a displays the cabinet inlet temperatures at different raised floor heights. It can be observed that as the floor height increases from 300 mm to 600 mm, the number of cabinets with high temperatures (indicated in red) significantly decreases, indicating a marked reduction in the average inlet temperatures of the cabinets, as well as a notable decrease in the range of temperature extremes. When the height exceeds 600 mm, fluctuations in inlet temperatures are observed, particularly at cabinet A14, which aligns with the fluctuations in temperature extremes shown in the simulations of Figure 15. However, the temperatures at other locations remain relatively unchanged, suggesting that when the height exceeds 600 mm, there is a limited ability to further reduce the inlet temperatures of the cabinets within the data center, and increasing the height does not affect the airflow distribution in the room.

Figure 16b illustrates the cabinet outlet temperatures at different raised floor heights. It can be observed that as the floor height increases from 300 mm to 600 mm, the number of cabinets indicated in red significantly decreases, suggesting an increase in the number of cabinets with lower average outlet temperatures, as well as a notable reduction in the range of temperature extremes. However, when the height exceeds 600 mm, fluctuations in outlet temperatures are observed, particularly at cabinet A14, which corresponds with the fluctuations in temperature extremes seen in the simulations of Figure 16a. In contrast, the temperatures at other locations remain largely unchanged, indicating that when the height exceeds 600 mm, the optimization effect on the airflow distribution is not significant.



(a) Temperature contours of cabinet inlets at different raised floor heights



(b) Temperature contours of cabinet outlets at different raised floor heights

Figure 16. Temperature contours of cabinet inlets and outlets at different raised floor heights.

4.1.4. Analysis of Evaluation Indicators at Different Raised Floor Heights

Using Equation (1), the Return Heat Index (RHI) was calculated based on the inlet and outlet temperatures of all cabinets in the data center at raised floor heights ranging from 300 mm to 800 mm, as shown in Figure 17. As the raised floor height increased, there was a notable rise in the RHI evaluation indicator for the data center. However, once the height reached 600 mm, the RHI remained relatively unchanged, indicating that the airflow distribution within the data center was no longer affected by the raised floor height at this point.

From the comprehensive analysis of airflow distribution optimization at different raised floor heights, it is evident that when the height reaches 600 mm, the airflow distribution within the data center is optimized. At this height, the airflow volume and static pressure distribution at the perforated floor grilles are more uniform; the pressure and velocity distributions beneath the raised floor are also more consistent; and the inlet and outlet temperatures of the cabinets are more evenly distributed, resulting in the smallest temperature differential. The evaluation indicator RHI also reaches its optimal value. Therefore, the 600 mm height of the raised floor is taken as the optimal choice, which is consistent with the optimal height recommended by Nada's study of air flow and thermal management in data centers [33]. Subsequent simulations set the raised floor height to 600 mm, which not only satisfies the requirements for airflow distribution in the data center but also contributes to a reduction in energy consumption.

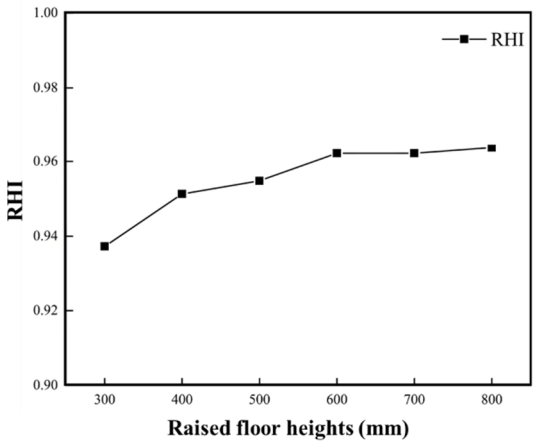


Figure 17. RHI indicators at different raised floor heights.

4.2. Closed Cold/ Hot Aisles

Enclosing the cold and hot aisles is the most effective strategy for enhancing cabinet cooling efficiency in data centers and is currently one of the most effective methods for retrofitting data centers. The closed cold aisle involves sealing the ends and top of the area formed by the perforated floor grille outlets and the cabinets, ensuring that all cold air flowing from the floor grilles is directed toward cooling the server cabinets. This air eventually returns through the cabinet exhaust to the air conditioning unit's return air inlet for processing. Conversely, the closed hot aisle involves sealing certain areas at the rear of the cabinet exhausts, directing the airflow that exits the back of the cabinets through return ducts to the return air inlet of the air conditioning unit. Enclosing the cold and hot aisles effectively prevents the mixing of hot and cold airflows, mitigating localized overheating in cabinets. By reducing the mixing of airflows and improving the cooling efficiency of the air conditioning system, this approach significantly enhances the Return Heat Index (RHI) values of the data center.

This study simulated four different operational conditions of airflow distribution in the data center: (1) neither the cold aisle nor the hot aisle is enclosed, (2) only the cold aisle is enclosed, (3) only the hot aisle is enclosed, and (4) both the cold and hot aisles are enclosed. Schematic diagrams of the enclosed cold and hot aisles are shown in Figure 18.

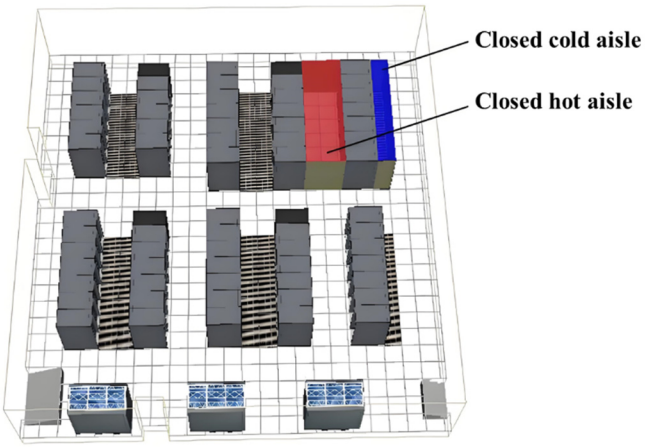
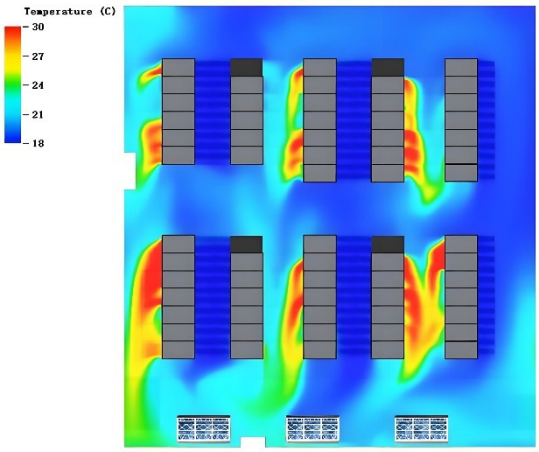


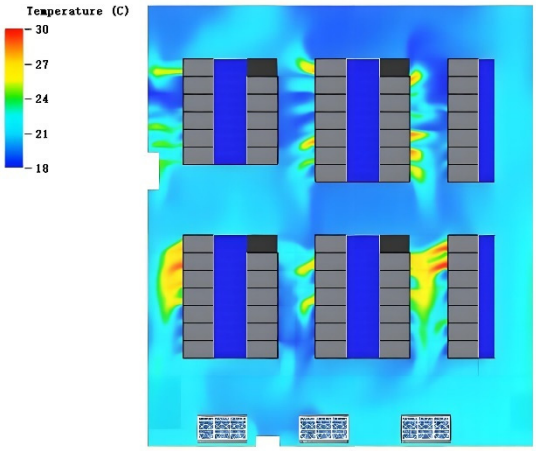
Figure 18. Schematic of the closed hot and cold aisles.

4.2.1. Analysis of the Temperature Field

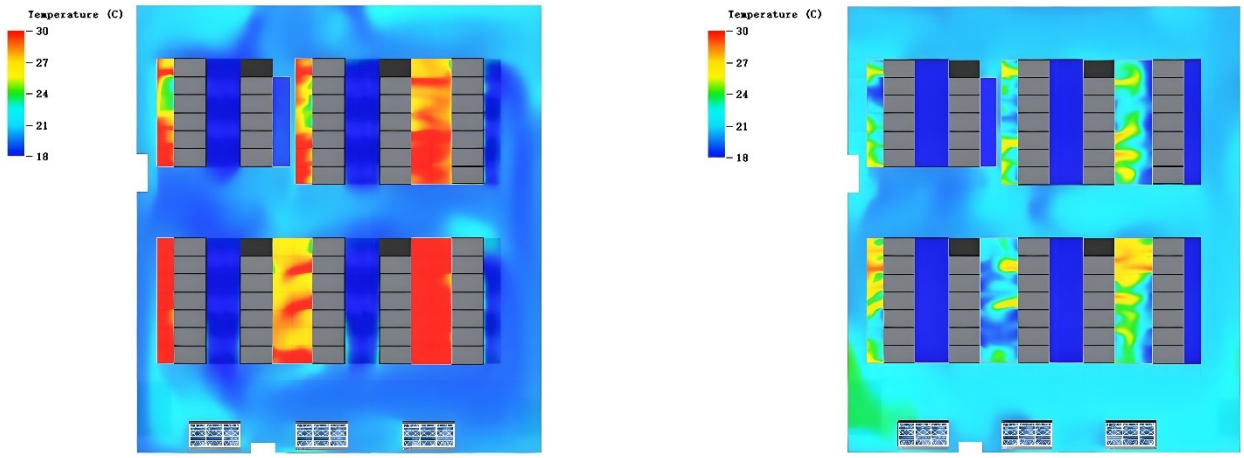
Figure 19 illustrates the temperature distribution at a height of 1.0 m within the data center under different aisle enclosure conditions. When neither the cold nor hot aisles are enclosed, the maximum temperature in the data center cross-section reaches 35 °C, while the minimum temperature is 18 °C, occurring at the cabinet inlets and outlets, thereby meeting the thermal environment design specifications for the data center. However, the mixing of supply and return airflow within the data center is quite pronounced, leading to localized overheating in some cabinets, which prevents the cooling capacity of the air conditioning units from being fully utilized for cabinet cooling, ultimately impacting the normal operation of the server equipment. Therefore, enclosing the cold and hot aisles in the data center can effectively isolate the supply and return airflow, reduce the mixing of hot and cold air, ensure adequate cooling of the server equipment, and improve the utilization of the cooling capacity of the air conditioning system, thus meeting the operational requirements for the thermal environment and airflow distribution within the data center.



(a) The hot and cold aisles are open



(b) Closed cold aisles



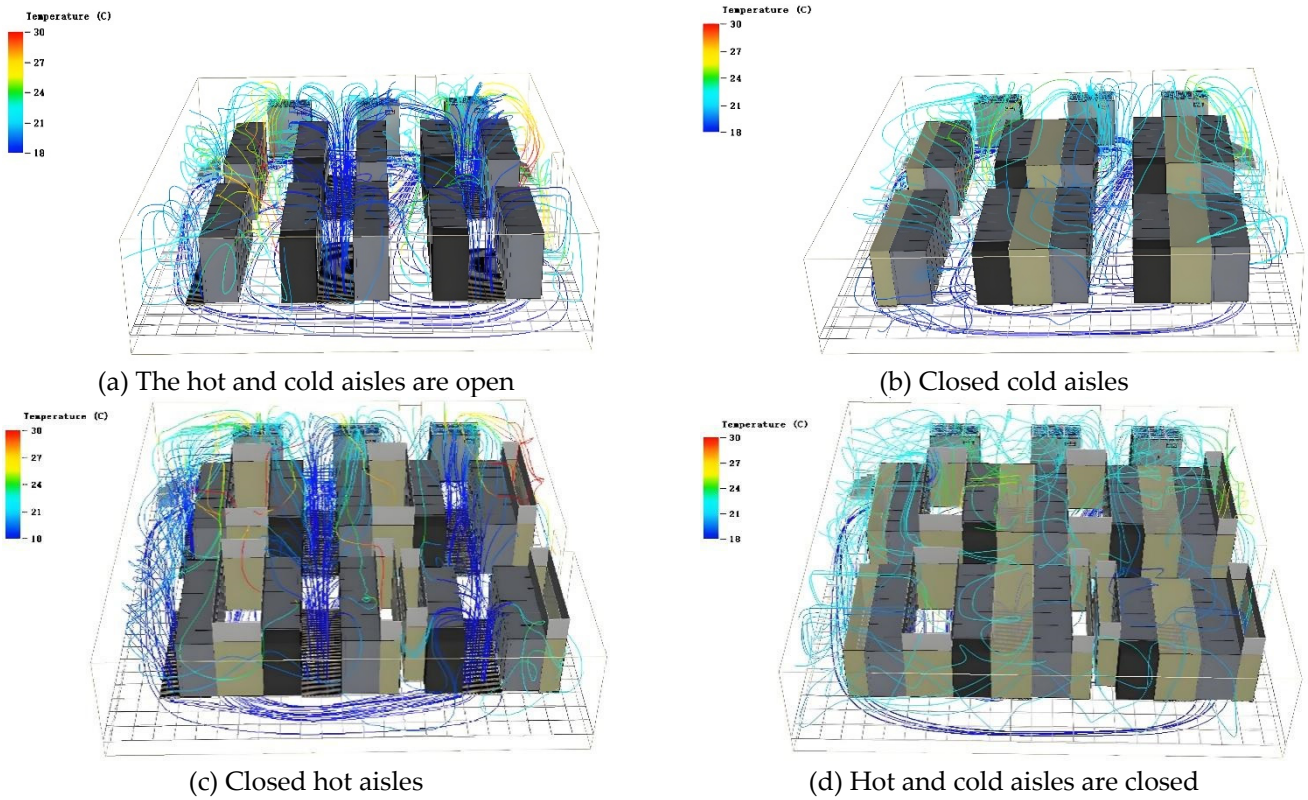
(c) Closed hot aisle (d) Hot and cold aisles are closed

Figure 19. Temperature contours distribution at 1.0 m horizontal height.

When the cold aisle of the data center is enclosed, as shown in Figure 19b, the mixing of supply and return airflow is reduced, effectively lowering the temperatures across various cross-sections of the data center. Under this condition, the average inlet temperature for the cabinets ranges from 18 °C to 18.4 °C, while the average outlet temperature is between 29 °C and 30 °C, indicating a significant reduction in the inlet and outlet temperatures of the cabinets and demonstrating the effectiveness of the cooling. Figure 19c illustrates the scenario when the hot aisle is enclosed; this method primarily reduces the mixing of hot and cold airflows. However, the enclosure of the hot aisle can lead to an increase in temperature at the cabinet outlets and data center hot aisle section, which generally remains at 30 °C but the highest temperature can reach 40.3 °C. Comparing the average temperatures of the data center and cabinets after enclosing both the cold and hot aisles reveals that enclosing the cold aisle creates a thermal environment for the cabinets that better meets operational requirements, with a more rational airflow distribution, higher utilization of cooling capacity, and improved cooling effectiveness. Thus, it can be concluded that enclosing the cold aisle provides a more favorable optimization effect compared to enclosing the hot aisle.

4.2.2. Streamline Analysis

Figure 20 presents the streamlines of the air conditioning units in the data center under four different operational conditions. The figure effectively reflects the distribution of supply and return airflow from the air conditioning system, as well as the variations in airflow temperature within the data center. It is evident from the figure that when the cold and hot aisles are not enclosed, significant mixing of hot and cold airflows occurs in the air conditioning system, leading to increased inlet temperatures for the cabinets, which is detrimental to the heat dissipation of the server equipment. After separately enclosing the cold and hot aisles, the airflow streamlines of the air conditioning system become clearer, with hot and cold airflows effectively isolated. The mixing of airflows is significantly improved, allowing the cooling capacity of the air conditioning system to be fully utilized for cooling the server equipment, resulting in an overall reduction in the temperature of the data center, enhanced airflow distribution, and increased efficiency of cooling capacity utilization.



(a) The hot and cold aisles are open (b) Closed cold aisles

(c) Closed hot aisles (d) Hot and cold aisles are closed

Figure 20. Streamlines of air conditioning system supply and return airflow.

By isolating the hot and cold airflows, cooling loss in the air conditioning system is reduced, allowing more cooling capacity to be directed toward actual equipment cooling, thereby enhancing the efficiency of cooling utilization. With improved cooling capacity utilization, air conditioning units can operate at lower loads while achieving the same cooling effect, leading to a reduction in energy consumption and operational costs. Enclosed aisles result in a more uniform temperature distribution, preventing the formation of hot spots and cold spots and improving the precision of temperature control within the data center.

4.2.3. Analysis of Evaluation Indicators Under Closed and Open Cold and Hot Aisles

After enclosing the cold and hot aisles, the Return Heat Index (RHI) is still used to evaluate the thermal environment of the data center, with the RHI values under different conditions shown in Table 3. From the table, it can be observed that the RHI evaluation indicator of the data center increased after the cold aisle was enclosed, while enclosing the hot aisle led to a decrease in the RHI indicator. This is because, when the hot aisle is enclosed, the air supply in the cold aisle directly flows to the air conditioning unit's return air inlet, resulting in a waste of cooling capacity. Therefore, enclosing the cold aisle proves to be more effective than enclosing the hot aisle. It is recommended that the layout of this data center utilize the closed cold aisle configuration.

Table 3. Evaluation indicators for whether to close hot or cold aisles.

Aisle Closed Condition	Q	δQ	RHI
Hot and cold aisles are open	811.9	863.8	0.9622
Closed cold aisles	599.9	617.8	0.9710
Closed hot aisles	810.9	874.7	0.9271
Hot and cold aisles are closed	679.0	680.7	0.9975

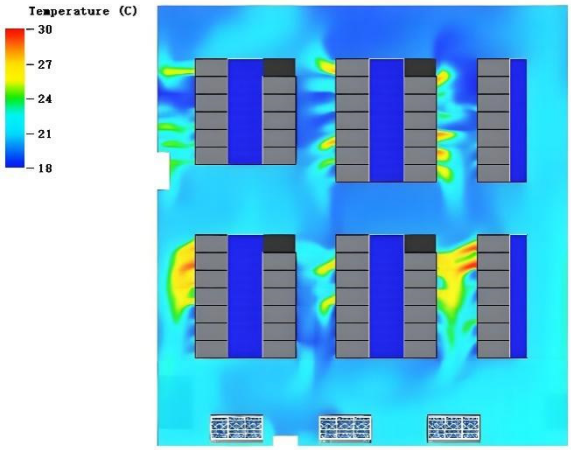
4.2.4. Impact of Increased Air Supply Temperature on Data Center Airflow Distribution

The study of closed aisles in the data center indicates that enclosing the cold aisle can significantly improve the airflow distribution within the facility. Lee et al. [34] noted that the temperature uniformity over the cold and hot aisles can result in the minor impacts of supply air temperature variations on the thermal performance indices for the large-scale data center [34]. In the aforementioned research, the air supply temperature from the air conditioning system was consistently maintained at 18 °C. Notably, after enclosing the cold aisle, the inlet temperature of the cabinets remained at 18 °C. Therefore, a simulation study was conducted to investigate the impact of increasing the air conditioning temperature after the cold aisle was enclosed on the cooling effectiveness of the data center.

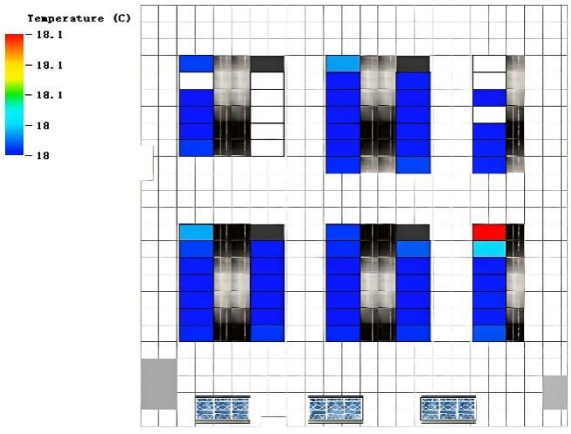
Figure 21 shows the temperature contours and average inlet temperature distribution for the cabinets at a height of 1.0 m above the floor with air supply temperatures of 18 °C and 20 °C. When the cold aisle of the data center is enclosed and the supply air temperature is raised to 20 °C, the average inlet temperature of the cabinets aligns with the air conditioning supply temperature, meeting the design requirements for cabinet inlet temperatures. The temperature distribution at a height of 1.0 m above the floor remains relatively unchanged, with only a slight increase in the outlet temperatures of the cabinets, primarily due to the elevated air supply temperature. However, the overall temperature distribution within the data center and the inlet and outlet temperatures of the cabinets all satisfy the design specifications. Therefore, when utilizing an enclosed cold aisle in the data center, it is feasible to moderately increase the air supply temperature within the design requirements to reduce the energy consumption of the air conditioning system.

The design of enclosed cold aisles helps optimize air flow paths, reduce the mixing of hot and cold air, and improve cooling efficiency. When the air supply temperature is moderately increased, it effectively reduces the load and energy consumption of the air conditioning system, while still meeting the design requirements for both the cabinet inlet temperature and the overall temperature distribution within the data center. This design optimization not only contributes to enhanced energy efficiency but also extends the equipment lifespan and improves the reliability of the data center.

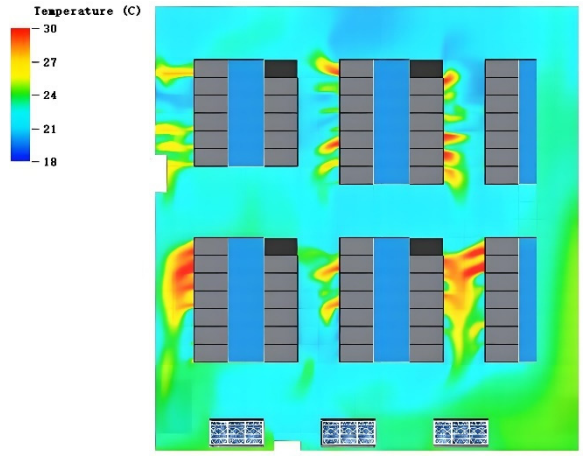
The simulation results indicate that after increasing the air supply temperature, there is a slight rise in the temperature distribution, with the average outlet temperature of the cabinets increasing from 33.2 °C to 33.8 °C, representing an increase of only 0.6 °C. The average inlet temperature of the cabinets rises from 18 °C to 20 °C. Therefore, when utilizing an enclosed cold aisle in the data center, to prevent waste of cooling capacity, the air supply temperature of the air conditioning system can be increased to 20 °C, thereby reducing the energy consumption of the data center's air conditioning system.



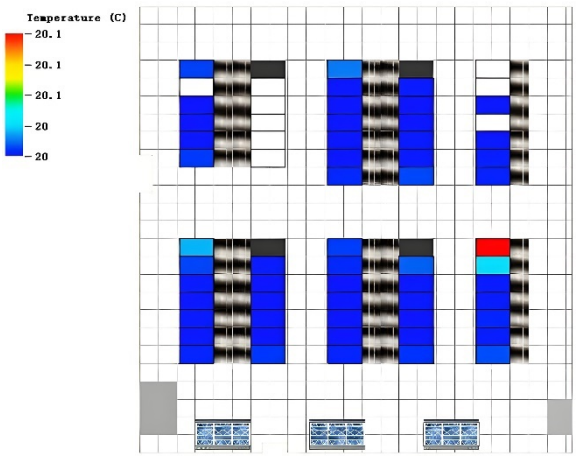
Temperature Contours of the Data Center at 1.0 m with Supply Air Temperature of 18 °C



Average Inlet Temperature Distribution of Cabinets with Supply Air Temperature of 18 °C



Temperature Contours of the Data Center at 1.0 m with Supply Air Temperature of 20 °C



Average Inlet Temperature Distribution of Cabinets with Supply Air Temperature of 20 °C

Figure 21. Temperature Contours of the Data Center at Different Air Supply Temperatures.

5. Conclusions

This study proposed airflow distribution optimization strategies through analyzing the problems of airflow distribution in an existing data center. The influence of a raised floor height and closed cold/hot aisles on the optimization airflow distribution were studied, and the results are as follows:

(1) When the height of the raised floor increased from 300 mm to 600 mm, the return heat index (RHI) in the data center significantly increased, indicating that the airflow distribution was effectively optimized. However, when the height of the raised floor exceeded 600, although the air volume, pressure, and RHI value increased, the changes were not significant. Considering the issue of space utilization in the computer room, the recommended height for a raised floor is 600 mm.

(2) An enclosed cold aisle significantly improved the RHI on the basis of raising the floor height by 600 mm, and cabinet average inlet and outlet temperature were 18–18.4 °C, 29–30 °C, respectively, indicating a significant cooling effect. When the hot aisles were closed, the highest temperature reached 40.3 °C, which is not conducive to heat dissipation.

(3) With a closed cold aisle, when the supply air temperature increased from 18 °C to 20 °C, the average outlet temperature of the cabinet only slightly increased from 33.2 °C to 33.8 °C (a minor temperature increase of 0.6 °C). Therefore, under the condition of an enclosed cold aisle in a data center, the supply air temperature can be appropriately increased within the design requirements to reduce the energy consumption of the air conditioning system.

Author Contributions: Conceptualization, F.Y. and H.C.; methodology, F.Y., H.C.; software, F.Y. and W.W.; validation, H.C., W.W. and J.A.; investigation, F.Y. and W.W.; writing—original draft preparation, F.Y.; writing—review and editing, H.C., W.W. and J.A.; supervision, H.C., W.W. and J.A. All authors have read and agreed to the published version of the manuscript.

Funding: This research was funded by Beijing Municipal Science and Technology Project, grant number Z231100006123014.

Data Availability Statement: The raw data supporting the conclusions of this article will be made available by the authors on request.

Conflicts of Interest: Author Wenqian Wang was employed by the company Capital Engineering & Research Invorporation Ltd. The remaining authors declare that the research was conducted in

the absence of any commercial or financial relationships that could be construed as a potential conflict of interest.

References

1. Lin, M.; Shao, S.; Zhang, X.; VanGilder, J.W.; Avelar, V.; Hu, X. Strategies for data center temperature control during a cooling system outage. *Energy Build.* **2014**, *73*, 146–152.
2. Chu, W.-X.; Wang, C.-C. A review on airflow management in data centers. *Appl. Energy* **2019**, *240*, 84–119.
3. Zhou, F.; Gu, W.; Ma, G. Advancements in data center cooling systems: From refrigeration to high performance cooling. *Energy Build.* **2024**, *320*, 114634.
4. Azarifar, M.; Arik, M.; Chang, J.-Y. Liquid cooling of data centers: A necessity facing challenges. *Appl. Therm. Eng.* **2024**, *247*, 123112.
5. Nada, S.A.; Elfeky, K.E.; Attia, A.M.A.; Alshaer, W.G. Experimental parametric study of servers cooling management in data centers buildings. *Heat Mass Transf.* **2017**, *53*, 2083–2097.
6. Cho, J.; Lim, S.-B. Balanced comparative assessment of thermal performance and energy efficiency for three cooling solutions in data centers. *Energy* **2023**, *285*, 129370.
7. Fulpagare, Y.; Bhargav, A.; Joshi, Y. Dynamic thermal characterization of raised floor plenum data centers: Experiments and CFD. *J. Build. Eng.* **2019**, *25*, 100783.
8. Tradat, M.I.; Sammakia, B.G.; Hoang, C.H.; Alissa, H.A. An experimental and numerical investigation of novel solution for energy management enhancement in data centers using underfloor plenum porous obstructions. *Appl. Energy* **2021**, *289*, 116663.
9. Meng, X.; Zhou, J.; Zhang, X.; Luo, Z.; Gong, H.; Gan, T. Optimization of the thermal environment of a small-scale data center in China. *Energy* **2020**, *196*, 117080.
10. Cho, J.; Woo, J. Development and experimental study of an independent row-based cooling system for improving thermal performance of a data center. *Appl. Therm. Eng.* **2020**, *169*, 114857.
11. Song, Z. Numerical investigation for performance indices and categorical designs of a fan assisted data center cooling system. *Appl. Therm. Eng.* **2017**, *118*, 714–723.
12. Moazamigoodarzi, H.; Pal, S.; Down, D.; Esmalifalak, M.; Puri, I.K. Performance of a rack mountable cooling unit in an IT server enclosure Therm. *Sci. Eng. Prog.* **2020**, *17*, 100395.
13. Cho, J. Numerical analysis of rack-based data center cooling with rear door heat exchanger (RDHx): Interrelationship between thermal performance and energy efficiency. *Case Stud. Therm. Eng.* **2024**, *63*, 105247.
14. Zhan, B.; Shao, S.; Zhang, H.; Tian, C. Simulation on vertical microchannel evaporator for rack-backdoor cooling of data center. *Appl. Therm. Eng.* **2020**, *164*, 114550.
15. Jiang, K.; Kheradmandi, M.; Hu, C.; Pal, S.; Yan, F. Data-driven fault tolerant predictive control for temperature regulation in data center with rack-based cooling architecture. *Mechatronics* **2021**, *79*, 102633.
16. Jin, C.; Bai, X.; Yang, C. Effects of airflow on the thermal environment and energy efficiency in raised-floor data centers: A review. *Sci. Total Environ.* **2019**, *695*, 133801.
17. Patankar, S.V. Airflow and cooling in a data center. *J. Heat Transf.* **2010**, *132*, 073001.
18. Zhang, M.; Zhang, Z.; Hu, Y.; Geng, Y.; Huang, H.; Huang, Y. Effect of raised floor height on different arrangement of underfloor air distribution performance in data center. *Procedia Eng.* **2017**, *205*, 556–564.
19. Song, Z. Numerical cooling performance evaluation of fan-assisted perforations in a raised-floor data center. *Int. J. Heat Mass Transf.* **2016**, *95*, 833–842.
20. Arghode, V.K.; Joshi, Y. Modeling Strategies for Air Flow Through Perforated Tiles in a Data Center. *IEEE Trans. Compon. Packag. Manuf. Technol.* **2013**, *3*, 800–810.
21. Ling, Y.Z.; Zhang, X.S.; Zhang, K.; Jin, X. On the characteristics of airflow through the perforated tiles for raised-floor data centers. *J. Build. Eng.* **2017**, *10*, 60–68.
22. Gao, T.; David, M.; Geer, J.; Schmidt, R.; Sammakia, B. Experimental and numerical dynamic investigation of an energy efficient liquid cooled chiller-less data center test facility. *Energy Build.* **2015**, *91*, 83–96.
23. Wang, T. The application of closed aisle in data room. *China Comput. Commun.* **2021**, *33*, 44–46.
24. Sundaralingam, V.; Arghode, V.K.; Joshi, Y.; Phelps, W. Experimental characterization of various cold aisle containment configurations for data centers. *J. Electron. Packag.* **2015**, *137*, 11007.
25. Manganelli, M.; Soldati, A.; Martirano, L.; Ramakrishna, S. Strategies for improving the sustainability of data centers via energy mix, energy conservation, and circular energy. *Sustainability* **2021**, *13*, 6114.

26. Zhang, Z.; Niu, B.; Zhang, Z.; Shi, M. Optimization on jet-induced ventilation to enhance the uniformity of airflow distribution in data center. *Energy Sci. Eng.* **2021**, *9*, 1973–1996.
27. Vasques, T.L.; Moura, P.; de Almeida, A. A review on energy efficiency and demand response with focus on small and medium data centers. *Energy Effic.* **2019**, *12*, 1399–1428.
28. Wang, L.; Wang, Y.; Bai, X.; Jin, Y.; Jiang, H.; Ma, Y. Optimization of thermal environment and airflow distribution in data center with row-based cooling using the Taguchi/TOPSIS method. *J. Build. Eng.* **2024**, *98*, 111415.
29. Lin, J.; Lin, W.; Lin, W.; Wang, J.; Jiang, H. Thermal prediction for Air-cooled data center using data Driven-based model. *Appl. Therm. Eng.* **2022**, *217*, 119207.
30. Cho, J.; Yang, J.; Park, W. Evaluation of air distribution system's airflow performance for cooling energy savings in high-density data centers. *Energy Build.* **2014**, *68*, 270–279.
31. Sharma, R.K.; Bash, C.E.; Patel, C.D. Dimensionless Parameters for Evaluation of Thermal Design and Performance of Large-scale Data Centers. In Proceedings of the 8th ASME/AIAA Joint Thermophysics & Heat Transfer Conferences, St. Louis, MO, USA, 24–26 June 2002.
32. Jin, S.Q.; Li, N.; Bai, F.; Chen, Y.J.; Feng, X.Y.; Li, H.W.; Gong, X.M.; Tao, W.Q. Data-driven model reduction for fast temperature prediction in a multi-variable data center. *Int. Commun. Heat Mass Transf.* **2023**, *142*, 106645.
33. Nada, S.A.; Said, M.A. Comprehensive study on the effects of plenum depths on air flow and thermal managements in data centers. *Int. J. Therm. Sci.* **2017**, *122*, 302–312.
34. Lee, Y.T.; Wen, C.Y.; Shih, Y.C.; Li, Z.; Yang, A.S. Numerical and experimental investigations on thermal management for data center with cold aisle containment configuration. *Appl. Energy* **2022**, *307*, 118213.

Disclaimer/Publisher's Note: The statements, opinions and data contained in all publications are solely those of the individual author(s) and contributor(s) and not of MDPI and/or the editor(s). MDPI and/or the editor(s) disclaim responsibility for any injury to people or property resulting from any ideas, methods, instructions or products referred to in the content.